Opioid and orexin hedonic hotspots in rat orbitofrontal cortex and insula

Daniel C. Castro[a,1] and Kent C. Berridge[b]

[a]Department of Anesthesiology, Washington University in St. Louis, St. Louis, MO 63108; and [b]Department of Psychology, University of Michigan, Ann Arbor, MI 48109

Hedonic hotspots are brain sites where particular neurochemical stimulations causally amplify the hedonic impact of sensory rewards, such as "liking" for sweetness. Here, we report the mapping of two hedonic hotspots in cortex, where mu opioid or orexin stimulations enhance the hedonic impact of sucrose taste. One hedonic hotspot was found in anterior orbitofrontal cortex (OFC), and another was found in posterior insula. A suppressive hedonic coldspot was also found in the form of an intervening strip stretching from the posterior OFC through the anterior and middle insula, bracketed by the two cortical hotspots. Opioid/orexin stimulations in either cortical hotspot activated Fos throughout a distributed "hedonic circuit" involving cortical and subcortical structures. Conversely, cortical coldspot stimulation activated circuitry for "hedonic suppression." Finally, food intake was increased by stimulations at several prefrontal cortical sites, indicating that the anatomical substrates in cortex for enhancing the motivation to eat are discriminable from those for hedonic impact.

opioid | affect | motivation | orbitofrontal cortex | insula

Positive hedonic reactions to pleasant events are important for normal affective function and well-being. By contrast, pathological hedonic dysfunction may contribute to depression, addiction, and other affect-related disorders. Underlying brain mechanisms include a network of discrete "hedonic hotspots" in subcortical nucleus accumbens (NAc) and ventral pallidum (VP) that can amplify hedonic impact of sensory pleasures, producing intense "liking" (1, 2). As yet, the role of cortex in causing hedonic enhancements remains unclear.

In favor of cortical contributions, neuroimaging studies have reported that human orbitofrontal cortex (OFC) and insula regions encode the pleasantness of palatable foods (3–6). For example, tasting palatable food elicits robust changes in cortical activity, and the intensity of pleasure-elicited cortical activity declines as individuals consume the food to fullness, corresponding to their decline of subjective pleasure ratings induced by growing satiety (i.e., alliesthesia) (3–6). However, the role of the cortex as necessary for "liking" is questioned by evidence that cortical damage usually does not cause loss of hedonic function: Lesions in the OFC, insula, or anterior cingulate cortex in humans do not reliably suppress positive hedonic reactions to many pleasant stimuli, despite causing cognitive impairments that alter decisions about selection, pursuit, and consumption of rewards (7–11). Similarly in animal studies, cortical lesions fail to strongly suppress reward-elicited behaviors (12–14).

Showing that the cortex causes gains of function in the motivation to consume food rewards, Mena et al. (15) recently reported that cortical mu-opioid stimulation in rats, via microinjections of DAMGO, a synthetic opioid agonist with high mu-opioid receptor selectivity, in the medial prefrontal cortex (PFC) produced robust increases of food intake. Here, we aimed to assess whether similar opioid stimulations in the prefrontal and insula cortex might also specifically cause increases in the hedonic impact of the sensory pleasure of food, as assessed by orofacial "liking" reactions to sweetness.

Beyond opioid stimulation, orexin stimulation has been found to similarly cause "liking" enhancements in the same NAc and VP hotspots where DAMGO enhances hedonic impact (16, 17),

raising the possibility that any cortical opioid hotspot for "liking" enhancement might also be stimulated by orexin. Orexin (hypocretin) is a hypothalamic peptide involved in appetite and in food and drug reward (18–20), beyond its role in arousal (21). Orexin neurons in hypothalamus project to PFC sites, including the OFC (22, 23), and orexin is a potential candidate to mediate hunger- and satiety-induced changes in "liking" (24, 25).

Therefore, we aimed here to compare orexin-A stimulation effects on "liking" reactions to those of opioid stimulation at the same cortical sites. We also compared the ability of opioid or orexin stimulations to alter the motivation to consume a sweet food. Finally, we compared patterns of Fos expression in reward circuitry throughout the brain recruited by cortical hotspot versus coldspot stimulations.

Results

Local Fos Plumes: Radius of Immediate Impact Surrounding Microinjections. To map the localization of function at cortical sites that altered "liking" reactions, we created Fos plume-based maps of the spread of the impact and affective effects of drug microinjections in the cortex (Figs. 1–3, 7, and 8). In these maps, the size of each microinjection symbol reflected the size of local Fos plumes induced by microinjections of DAMGO or orexin, as reflected by Fos expression in neurons surrounding a microinjection site (Fig. 1). The color of each map symbol was determined by the within-subject behavioral effects of drug microinjections caused at that site on hedonic taste reactions, or on food intake, relative to baselines measured after vehicle microinjections in the same rats.

To assess the size of Fos plumes, a separate group of rats received only one microinjection of DAMGO, orexin, or vehicle. That is, local Fos expression surrounding a DAMGO microinjection or
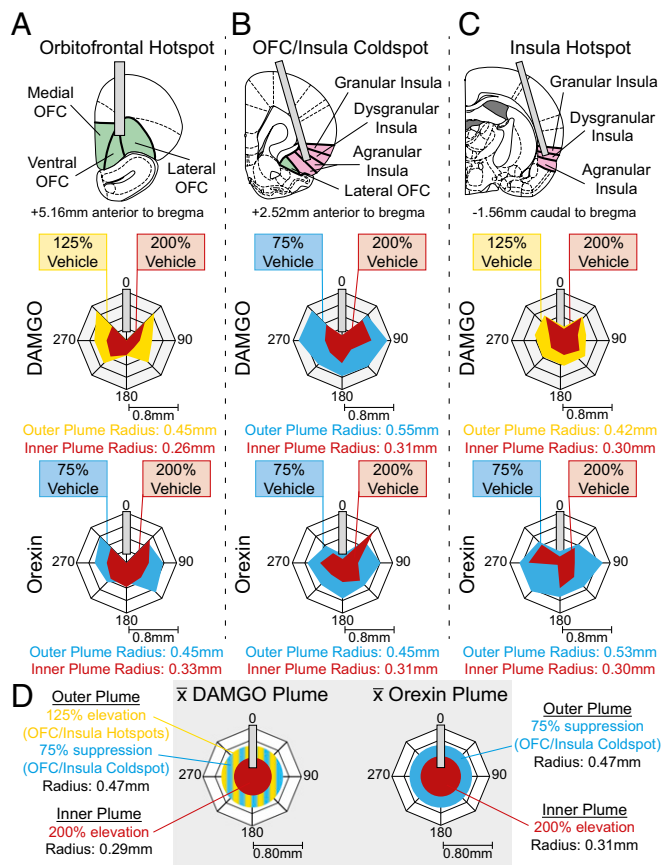
Fig. 1. Microinjection Fos plumes. Fos plumes were mapped around DAMGO and orexin microinjections at three sites in the cortex: the OFC hotspot (*A*), the OFC/insula coldspot (*B*), and the insula hotspot (*C*). DAMGO produced excitatory outer plumes in the rostral OFC and caudal insula but an inhibitory outer plume in the OFC/insula middle zone and excitatory inner plumes in all three sites. Orexin produced similar inhibitory outer and excitatory inner plumes at all three sites. Drug-induced radius and percent intensity change in Fos from vehicle microinjections are shown for DAMGO and orexin microinjections. (*D*) Sizes of plumes used for symbol mapping; these sizes were stable across cortical sites. DAMGO: outer plume: $F_{(2,23)} = 2.967$, $P = 0.073$; inner plume: $F_{(2,23)} = 0.311$, $P = 0.736$; orexin: outer plume: $F_{(2,18)} = 0.659$, $P = 0.531$; inner plume: $F_{(2,23)} = 0.086$, $P = 0.918$.

an orexin microinjection in some rats was compared with control levels measured in other rats that received vehicle microinjections at comparable sites. A single-microinjection group was used for plume size assessment to avoid potential shrinkage of plumes after repeated microinjections due to gliosis or damage, which would lead to false underestimation of size (26). Fos plume size and Fos intensity were measured separately for rostral vs. caudal subregions of the OFC and insula in case those regions differed in Fos responsiveness to drug microinjections (Fig. 1 and Fig. S1).

We did detect some regional differences in Fos plumes across different cortical sites. For example, DAMGO microinjections in the rostral OFC and caudal insula generated large outer plumes with radii of 0.42–0.45 mm where Fos was increased by 125% over vehicle-induced levels. Rostral OFC and caudal insula plumes contained an inner intense excitatory plume with 0.26- to 0.31-mm radii, where Fos was elevated by 200% over vehicle control levels (volume = 0.07–0.13 mm^3). In the rostral insula, DAMGO microinjections oppositely reduced Fos by 25% below vehicle (i.e., an inhibitory antiplume) in a similarly sized outer plume with a radius of 0.55 mm. DAMGO stimulation still caused a 200% increase in Fos in a smaller inner plume with a radius of 0.31 mm. Since the size of these plumes did not differ

significantly across the OFC and insula subregions, but only in the direction of change for outer plumes, their radius averages were taken to produce a single DAMGO symbol size for maps: an outer radius of 0.47 mm (volume = 0.44 mm^3) and an inner radius of 0.29 mm (volume = 0.10 mm^3). That symbol size was used for all DAMGO symbols in functional maps of taste reactivity and of food intake (Figs. 2 and 7).

For orexin-induced Fos plumes, microinjections in the OFC and insula also reliably generated plumes of similar size at all cortical sites but with a different center–surround organization. Orexin Fos plumes all contained an inner excitatory center where Fos was elevated by 200% over vehicle control levels with a radius of 0.31 ± 0.01 mm (volume = 0.13 ± 0.02 mm^3), surrounded by an outer inhibitory antiplume where Fos was suppressed by 25% below control vehicle levels (radius 0.48 ± 0.03 mm; volume = 0.46 ± 0.08 mm^3). These plume sizes were used to set the diameters of orexin microinjection symbols in all functional maps (Figs. 3 and 8).

Hedonic Impact: Anterior OFC Contains an Opioid–Orexin Hedonic Hotspot. An opioid hedonic hotspot was found in an 8-mm^3 subregion of the rostromedial OFC: In this OFC site DAMGO microinjections enhanced by 200–300% the number of positive hedonic ("liking") reactions elicited by sucrose taste (compared with control levels elicited by sucrose in the same rats after vehicle microinjections) (Fig. 2).

Orexin microinjections in this rostromedial OFC hotspot similarly doubled to tripled the positive hedonic reactions elicited by sucrose (Fig. 3 and Figs. S2 and S3). Therefore, this rostromedial OFC site was considered to be a hedonic hotspot shared by both opioid and orexin mechanisms for "liking" enhancement. Both drugs in this OFC site elevated the entire constellation of positive hedonic reactions—rhythmic tongue protrusions, lateral tongue protrusions, and paw licks—as a group (Figs. S3 and S4). This pattern suggests hedonic amplification rather than motor effects on a single reaction. By contrast, neither DAMGO nor orexin microinjections altered negative "disgust reactions" elicited by quinine (i.e., gapes, headshakes, forelimb flails, chin rubs, or paw treads). The failure to alter bitterness-elicited disgust reactions also helps rule out general sensorimotor or arousal changes and suggests that OFC affective modulation was restricted to the positive hedonic dimension for sweetness "liking". Finally, opioid/orexin hedonic enhancement also appeared to require actual concomitant sucrose sensation, as no orofacial reactions were spontaneously emitted by rats that had received DAMGO or orexin microinjections in the absence of sucrose oral infusion. This pattern also seems to rule out simple motor effects on orofacial reactions.

Anatomically, the anterior border of the rostromedial OFC hedonic hotspot began near the rostral edge of the medial orbital and ventral orbital cortex. Medially, the OFC hotspot extended posteriorly along the midline of the brain to the posterior border of the medial orbital cortex. However, the hedonic hotspot did not penetrate prelimbic, infralimbic, or anterior cingulate regions of the medial PFC: DAMGO or orexin microinjections at these sites generally failed to alter sucrose-elicited reactions. Speculatively extrapolating to humans, this pattern suggests that the medial portion of the OFC hotspot might correspond roughly to human area 14 (caudal), located immediately rostral to prelimbic area–area 32d (27). However, although prelimbic cortex microinjections failed to increase hedonic reactions, orexin (but not DAMGO) microinjections in the prelimbic cortex did decrease disgust reactions to quinine ($\chi^2 = 9.33$, $P = 0.009$; DAMGO: $Z = -0.312$, $P = 0.755$; orexin $Z = -2.319$, $P = 0.020$), suggesting a potential but slightly different role in suppressing negative affect (Fig. S5).

Along the lateral surface of the brain, the OFC hedonic hotspot extended posteriorly through the entire ventral orbital area (potentially corresponding to area 13) and through the anterior two-thirds of the ventral lateral orbital area of the OFC to the claustrum
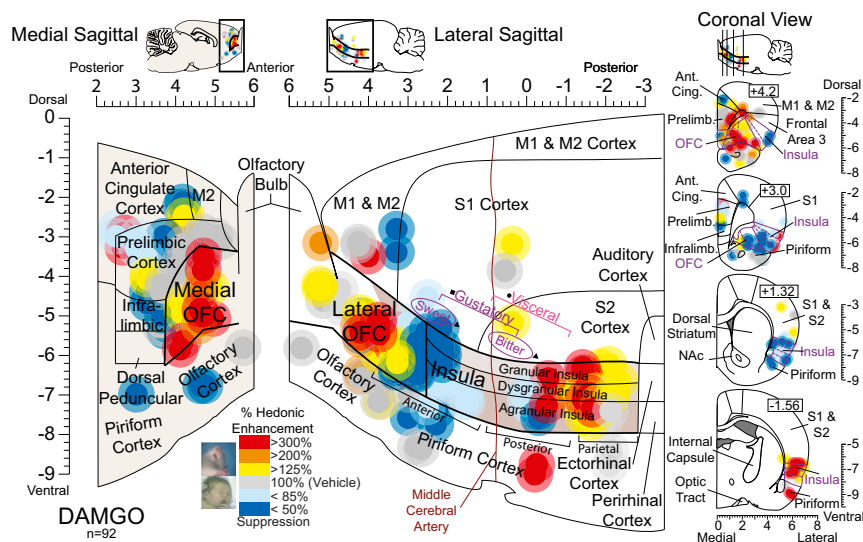
Fig. 2. Mu-opioid stimulation alters the hedonic impact of sucrose at cortical sites. Functional maps show hedonic effects of DAMGO microinjections at each cortical site on taste reactivity ("liking" reactions) elicited by sucrose taste. Each symbol placement indicates an individual rat's microinjection site (symbol size reflects the DAMGO Fos plume). Symbol colors reflect the within-subject behavioral change in hedonic reactions induced by DAMGO microinjection, shown as percentage change from vehicle control levels measured in the same rat (hedonic enhancements: yellow–orange–red; suppressions: blue). Mu-receptor stimulation effects by DAMGO microinjection in the OFC enhanced hedonic "liking", depending on the anatomical subregion of the OFC (rostromedial versus caudolateral OFC: $\chi^2 = 4.967$, $P = 0.026$). At rostromedial sites, DAMGO stimulation enhanced hedonic "liking" reactions to sucrose by 200–300% [$\chi^2 = 15.826$, $P < 0.001$; DAMGO: $Z = -2.983$, $P = 0.003$, $r = -0.81$, CI (2, 12); $n = 13$]. DAMGO microinjections in the caudolateral OFC and rostral 2/3 of insula oppositely suppressed hedonic reactions [$\chi^2 = 17.659$, $P < 0.001$; DAMGO: $Z = -3.673$, $P < 0.001$, $r = 0.65$, CI (−9, −2); $n = 26$]. DAMGO microinjections in the far-caudal insula enhanced hedonic reactions compared with vehicle baseline [vehicle: $\chi^2 = 9.75$, $P < 0.008$; DAMGO: $Z = -2.524$, $P = 0.012$, $r = 0.63$, CI (1, 11); $n = 11$] and compared with DAMGO at rostral/mid sites in the insula ($\chi^2 = 34.320$, $P < 0.0001$). No other cortical site altered hedonic reactions (gray; $n = 42$). Functional insula zones are based on Kosar et al. (51) (square), Cechetto and Saper (28) (circle), and Peng et al. (45) (triangle).

(hotspot posterior border ∼ +3.5 mm anterior to Bregma and lateral border ∼ ±3.0 mm lateral to midline, corresponding to area 12/47). By contrast, an oppositely valenced hedonic coldspot, described below, occupied the most posterior one-third of the ventrolateral orbital area and posteriorly beyond, where sucrose-"liking" reactions were reduced by DAMGO or orexin microinjections.

In total extent, the dimensions of the OFC hotspot were estimated to be anteroposterior (A–P) length = 2.9 mm (including both the medial surface and the lateral surface); mediolateral (M–L) width = 1.8 mm; and dorsoventral (D–V) height = 1.63 mm (Figs. 1 and 2). The total volume of the OFC hotspot was thus calculated to be ∼8.5 mm³. However, we note our sites did not probe into the dorsal region of the lateral orbital area, leaving it uncertain whether the hotspot's anterior dorsolateral edge extended there. The dimensions and volumes above were calculated based on all sites where our microinjections were found to exert positive "liking" effects.

Suppressive Lateral Coldspot: Posterior OFC and Most of the Insula.
Immediately posterior to the OFC hotspot, an oppositely valenced hedonic coldspot or strip was mapped along the ventrolateral surface of the brain, stretching over 5 mm in A–P length from the caudal OFC through most of the insula. In this suppressive strip, DAMGO or orexin microinjections cut in half the number of positive hedonic orofacial reactions elicited by sucrose compared with vehicle levels in the same rats (33–50% suppression) (Figs. 2 and 3 and Fig. S3). The suppressive coldspot filled the posterolateral OFC and continued posteriorly through all the anterior, middle, and even part of the posterior insula (Figs. 2 and 3).

Within the anterior/middle insula, suppressive sites were equally distributed across agranular, dysgranular, and granular zones of insula cortex. The coldspot continued ventrally to the piriform cortex and endopiriform nucleus and dorsally to claustrum above the OFC, frontal cortex (area 3), and somatosensory cortex above the insula. Its medial boundary was the ventral claustrum, the infralimbic cortex (area 25), and the dorsal pe-

duncular cortex. The total dimensions of the OFC–insula coldspot for both DAMGO and orexin were 5.51 mm A–P, 2.06 mm M–L, and 1.55 mm D–V, generating a total volume of 18 mm³.

Posterior Hedonic Hotspot in Far-Caudal Insula. A second cortical hedonic hotspot was identified in the far-posterior insula. The anterior edge of this posterior insula hotspot began immediately behind the caudal edge of the coldspot, essentially filling the far-posterior 25% of insula (i.e., near parietal cortex). In this posterior insula hotspot, microinjections of either DAMGO or orexin again doubled or tripled the number of hedonic reactions elicited by sucrose compared with vehicle control levels in the same rats (Figs. 2 and 3 and Fig. S3). Opioid and orexin hedonic enhancements were again selective to positive hedonic "liking" reactions elicited by sucrose: Neither opioid nor orexin altered the robust disgust gapes and related negative reactions elicited by quinine ($\chi^2 = 4.769$, $P = 0.092$) (Fig. S4). Hedonic enhancements again required simultaneous sucrose infusion to be observed and did not occur as anticipatory reactions before the onset of sucrose infusions.

Anatomically, the anterior edge of the insula hedonic hotspot was approximately at −0.5 mm Bregma, an A–P level where the fornix diverges medially into bilateral columns and where the anterior edge of third ventricle and the posterior edge of anterior commissure are also located. The insula hotspot extended posteriorly over 2 mm, ending at the border of the perirhinal and ectorhinal cortex. Thus, this hotspot included posterior insula sites traditionally viewed as having sensory visceral and respiratory functions (28, 29). Dorsally, the insula hedonic hotspot extended to the secondary somatosensory cortex and ventrally to the piriform cortex. Medially, the hotspot was bordered by the claustrum rostrally and the external capsule caudally. Agranular, dysgranular, and granular layers of the far-posterior insula again all contained roughly equal proportions of hedonic enhancement sites. The dimensions of the hedonic hotspot in posterior insula stretched 2.7 mm A–P in length, 1.41 mm M–L in width, and
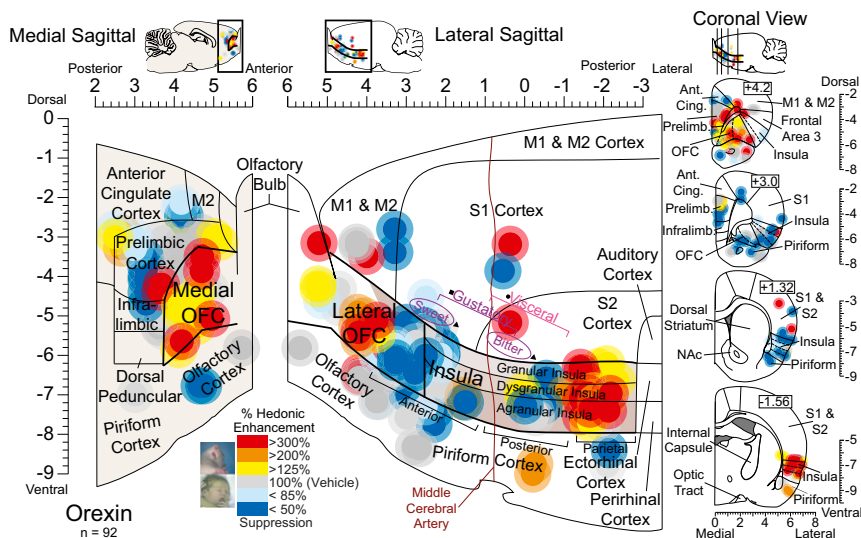
Fig. 3. Orexin stimulation alters hedonic impact in localized sites in the cortex. Functional maps show the effects of orexin microinjections at cortical sites on hedonic reactions to sucrose. Symbol logic is identical to Fig. 2 (enhancements: yellow–orange–red; suppressions: blue). Orexin stimulation at rostromedial sites enhanced hedonic "liking" reactions to sucrose by 200–300% [χ^2 = 5.73, P = 0.017; Z = −2.519, P = 0.012, r = −0.76, CI (1, 16)]. Orexin microinjections in the caudolateral OFC and the rostral two-thirds of the insula oppositely suppressed hedonic reactions by 33–50% [Z = −2.723, P = 0.006, r = 0.55, CI (−9, 0)]. Orexin microinjections in the far-caudal insula enhanced hedonic reactions compared with vehicle baseline [Z = −2.386, P = 0.017, r = 0.60, CI (1, 22)]. No other cortical site altered hedonic reactions to sucrose statistically (medial PFC: χ^2 = 0.559, P = 0.756; cingulate: χ^2 = 0.667, P = 0.717; prelimbic: χ^2 = 0.744, P = 0.689; infralimbic: χ^2 = 2.923, P = 0.232; olfactory: χ^2 = 1.733, P = 0.42; piriform: χ^2 = 1.067, P = 0.587; sensory/motor: χ^2 = 0.364, P = 0.834).

1.47 mm D–V in height. The total volume of the insula hotspot was 5.70 mm³ based on these dimensions.

Comparison of DAMGO/Orexin Effects in OFC/Insula Hotspots vs. the Coldspot. The hedonic function map described above suggests that the two opioid/orexin hedonic hotspots in the rostral OFC and posterior insula essentially bracket the hedonic coldspot strip between them (Figs. 1 and 2). DAMGO and orexin shared the same anatomical hotspot boundaries, and within those boundaries the neurochemical stimulations produced comparable effects (Z = −0.915, P = 0.374) (Figs. 1 and 2). Similarly, in the 5-mm coldspot both drugs produced hedonic suppressions (posterior OFC, anterior insula, and mid to posterior insula) (DAMGO Z = −0.661, P = 0.539; orexin Z = −0.166, P = 0.872), although DAMGO produced a slightly stronger suppression (64% DAMGO vs. 79% orexin; Z = −2.117, P = 0.034).

Distant Fos in Subcortical Structures Induced by Cortical Hotspot vs. Coldspot Microinjections. We assessed distant changes in Fos expression in cortex and in several subcortical structures recruited by cortical hotspot/coldspot microinjections of DAMGO or orexin, focusing on the NAc shell, VP, and lateral hypothalamus (Figs. 4–6, Fig. S1, and Tables S1–S3). For all structures, Fos was measured after initial DAMGO/orexin microinjections in the cortex and was compared with control Fos levels measured in other rats after vehicle microinjections at the same cortical site. The effects on Fos of cortical drug microinjections alone (without taste infusions) were used to avoid confounds by motor/behavioral feedback effects on Fos expression that would accompany taste-elicited orofacial reactions and to obtain a pure site comparison of neurochemical stimulation effects.

OFC hotspot microinjections. DAMGO or orexin microinjections in the rostral OFC hotspot each recruited an increase in Fos expression in the posterior insula hotspot by >15% (orexin) to >25% (DAMGO) over vehicle control levels, suggesting the two cortical hotspots were coactivated. By contrast, no Fos increase was seen in the cortical OFC/insula coldspot after rostral OFC hotspot drug microinjections (Fig. 4). Subcortically, DAMGO or orexin microinjection in the OFC hotspot also recruited increases of >50% Fos expression in the medial shell of the NAc and specifically in its rostrodorsal quadrant that has been previously identified as containing a NAc hedonic hotspot (16, 26, 30). By contrast, no NAc increase in Fos was found in either rostroventral or caudal (coldspot) subregions of the medial shell (26). Finally, microinjections of DAMGO/orexin in the rostral OFC hotspot also recruited

a >25% Fos increase in the lateral hypothalamus at the site containing orexin cell bodies.

Posterior insula hotspot microinjections. DAMGO microinjections in the hedonic hotspot of the far-posterior insula did not detectably alter Fos in the rostromedial OFC hotspot, but orexin microinjections did recruit >25% increases of Fos in the rostral OFC hedonic hotspot as well as in the OFC/insula coldspot strip (all with effect sizes of Cohen's d >1.0). Subcortically, both DAMGO and orexin microinjections in insula hotspot recruited increases of >15% in Fos expression in the anterior and posterior halves of the VP (d >0.7 to >1.0). Orexin (but not DAMGO) microinjections also recruited a >25% Fos increase in the NAc hedonic hotspot of the rostrodorsal medial shell (no changes in the rostroventral shell or in the caudal shell coldspot). In the VP, the caudal half has previously been identified to contain an opioid/orexin hedonic hotspot, whereas the rostral half contains an opioid coldspot for suppression of "liking" reactions to sucrose taste (17, 31). However, the caudal VP is also implicated in positive incentive motivation for drug and food rewards (Fig. 5) (31, 32). Finally, DAMGO microinjection in the posterior insula hotspot suppressed Fos by >25% in a NAc hedonic coldspot in the caudal medial shell (i.e., produced Fos levels that were <75% of control vehicle-microinjection levels at the same site) (Fig. 5).

These results suggest that opioid/orexin stimulations of the far-posterior insula hotspot may recruit widespread "hedonic circuitry" similar to that recruited by stimulations of the anterior OFC hotspot and may suppress opposing antihedonic circuitry. Overall this pattern suggests that OFC and insula hotspots can each recruit hedonic-enhancing circuitry that is widely spread throughout the brain, potentially as part of a larger mechanism for cortically mediated enhancement of "liking" reactions.

OFC–insula coldspot microinjections. In the hedonic coldspot zone stretching from the posterior OFC through the anterior and middle insula, where stimulations suppressed sucrose-"liking" reactions, DAMGO or orexin microinjections produced a cross-cortical >25% suppression of Fos in the rostral OFC hedonic hotspot (Fig. 6). However, the far-posterior insula hotspot was not detectably altered. Subcortically, insula coldspot microinjections of DAMGO and orexin both produced >25% suppression in the lateral hypothalamus. Conversely, insula coldspot stimulations produced a >25% (DAMGO) to >50% (orexin) increase in Fos in both the NAc opioid coldspot in the caudal medial shell and in the VP coldspot in the anterior VP (effect size d >1.0). Cross-coldspot activation suggests the recruitment of a distributed antihedonic network that might participate in reducing "liking" reactions to
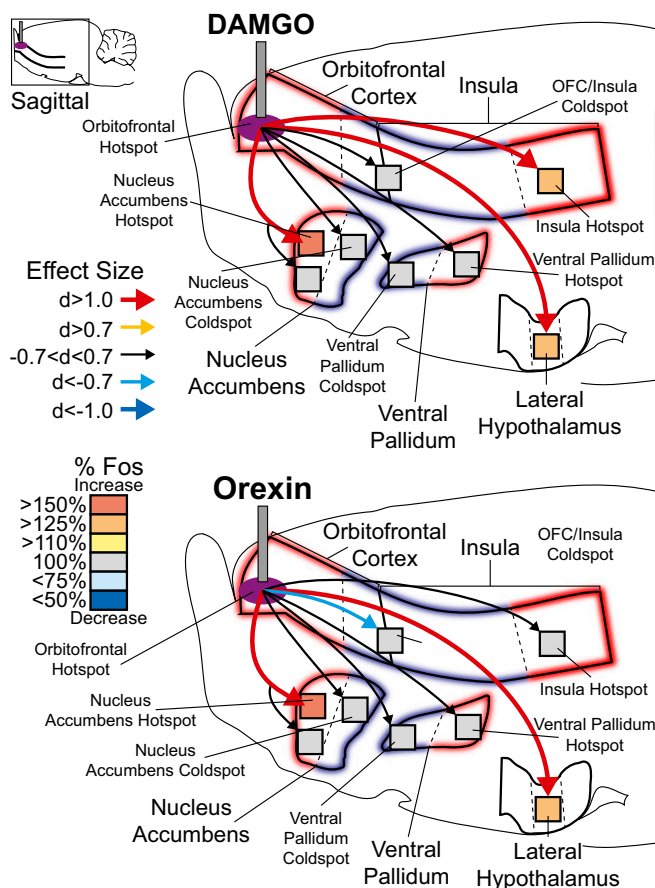
Fig. 4. OFC hotspot stimulation recruits larger brain circuitry for hedonic enhancement. (*Upper*) DAMGO microinjections in the OFC hotspot increased Fos by >130% in the insula hotspot ($d = 3.34$) relative to vehicle microinjections (vehicle = 100%). No change was detected in the cortical coldspot ($d = -0.477$). Subcortically, DAMGO microinjection in the OFC hotspot increased Fos in the rostrodorsal NAc medial shell hotspot by >250% ($d = 4.02$) but did not alter Fos in the rostroventral NAc ($d = -0.160$) or in the NAc caudal coldspot ($d = 0.041$). DAMGO microinjection in the OFC hotspot did not change Fos in the VP caudal hotspot ($d = 0.00$) or VP rostral coldspot ($d = -0.199$) but did increase Fos by 125% in the mid perifornical lateral hypothalamus ($d = 2.37$). Orexin microinjections in the OFC hotspot mildly reduced Fos in the caudal OFC and insula coldspot by 15% below baseline ($d = -0.741$) and mildly increased Fos by 113% in the far-caudal insula hotspot ($d = 0.612$) relative to vehicle injections. Like DAMGO, orexin microinjection in OFC hotspot also increased Fos in the NAc rostrodorsal shell hotspot by 180% ($d = 1.26$) but did not alter Fos in the rostroventral NAc ($d = -0.131$) or the caudal shell coldspot ($d = -0.325$). Orexin microinjection in OFC hotspot did not change Fos in the VP caudal hotspot ($d = 0.528$) or rostral coldspot ($d = -0.288$) but did increase Fos in the lateral hypothalamus by 128% ($d = 1.66$).

sucrose to below-normal levels (Fig. 6) (26, 33, 34). However, orexin (but not DAMGO) also recruited a similar Fos increase in the caudal VP, which contains the VP hedonic hotspot and so is less easily explained as hedonic suppression.

OFC and Insula Affect Food Intake Differently. The intake of palatable sweet food (M&M chocolate candies) was measured in 1-h free-intake tests conducted immediately after each taste-reactivity session. We found that palatable food intake was increased by 30–70% after DAMGO microinjection at virtually all OFC sites in both the hedonic hotspot and coldspot subregions (although tending highest at rostral OFC sites) compared with vehicle microinjections in the same rats (Fig. 7). This supports the report by Mena et al. (15) that DAMGO stimulations at higher doses enhanced food intake in sites throughout the entire

OFC and beyond. These sites extended beyond our OFC hedonic hotspot to additional OFC and other prefrontal sites, which might be viewed as inducing increased "wanting" to eat without increasing "liking" for what is eaten (15, 35). Different physical stimuli were used for our taste-reactivity test (sucrose solution) and food intake test (sucrose-containing chocolate candy). We view that difference as unlikely to contribute much to the difference between our hedonic vs. intake cortical maps, given that Mena et al. also reported that two physically different foods gave similar intake results. By contrast, we did not observe increases in food intake after either DAMGO or orexin microinjections at sites in the prelimbic, infralimbic, or anterior cingulate cortex (Figs. 6 and 7). This is different from the increased food intake reported by Mena et al. (15), but we note our DAMGO dose was only 1/20th of their most
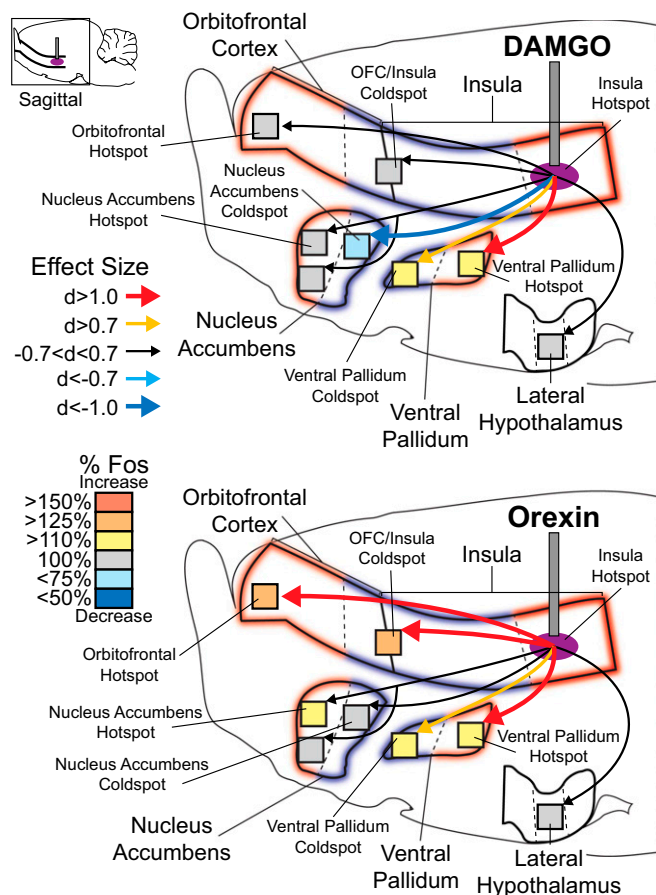

Fig. 5. Insula hotspot stimulation recruits larger brain circuitry for hedonic enhancement. DAMGO microinjections in the far-caudal insula hotspot did not alter Fos in the rostral OFC hotspot ($d = 0.565$), in the OFC/insula coldspot ($d = 0.308$), in the NAc rostrodorsal shell hotspot ($d = 0.068$), or in the rostroventral NAc ($d = -0.128$) but caused 32% suppression of Fos in the NAc caudal shell coldspot ($d = -1.605$). DAMGO microinjections in the far-caudal insula hotspot also increased Fos in the VP hotspot by 122% ($d = 1.4$) and in the VP coldspot by 118% ($d = -0.94$). Unlike DAMGO stimulation of the OFC hotspot, insula hotspot stimulation did not alter Fos in the lateral hypothalamus ($d = -0.409$). In contrast to DAMGO stimulation, orexin microinjection in the far-caudal insula hotspot increased Fos in both the rostral OFC hotspot (elevation = 133%; $d = 1.2$) and OFC/insula coldspot (elevation = 143%; $d = 2.06$). Orexin microinjection in the far-caudal insula hotspot also mildly increased Fos by 121% in the NAc rostrodorsal shell hotspot ($d = 0.669$) but did not increase Fos in the rostroventral NAc shell ($d = -0.128$) or NAc caudal shell coldspot ($d = -0.57$). Orexin microinjection in the far-caudal insula hotspot elevated Fos to 114% in the caudal VP hotspot (elevation =; $d = 1.14$) and to 112% in rostral VP coldspot ($d = 0.564$), and, like DAMGO, did not alter Fos in the lateral hypothalamus ($d = 0.0$).
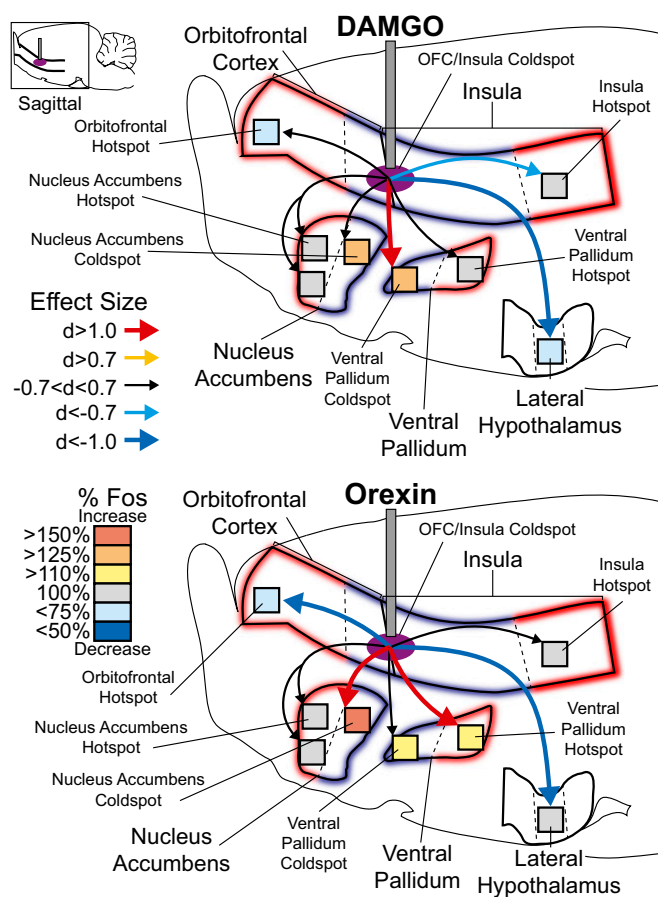
Fig. 6. Mu-opioid or orexin stimulation in OFC/insula coldspot recruits distinctive circuitry for hedonic suppression. DAMGO stimulation in the OFC/insula coldspot suppressed Fos by 27% below vehicle in the rostral OFC hotspot ($d = -0.682$) and suppressed Fos by 21% in the far-caudal insula hotspot ($d = -0.762$) relative to vehicle microinjection levels (vehicle = 100%). DAMGO stimulation in the OFC/insula coldspot did not alter Fos in the NAc rostrodorsal shell hotspot or rostroventral shell but did increase Fos in the caudal shell NAc coldspot by 125% ($d = 0.531$). Fos activity in the caudal VP hotspot was not changed ($d = 0.154$), but Fos was increased 138% in the rostral VP coldspot ($d = 1.172$) and was suppressed 24% in the lateral hypothalamus ($d = -2.025$). By comparison, orexin microinjection in the OFC/insula coldspot robustly suppressed Fos activity by 34% in the OFC hotspot ($d = -1.102$) but left the insula hotspot unaltered ($d = 0.608$). Orexin microinjection in the OFC/insula coldspot did not change Fos in the NAc rostrodorsal shell hotspot or in the rostroventral shell but did increase Fos by 152% in the NAc caudal shell coldspot ($d = 1.164$). Orexin microinjection in the OFC/insula coldspot also increased Fos by 124% in the VP caudal hotspot ($d = 1.142$) and by 120% in VP rostral coldspot ($d = 0.684$). Finally, orexin microinjections in the OFC/insula coldspot suppressed Fos activity by 20% in the lateral hypothalamus ($d = -1.174$).

effective dose. There were also differences in test procedures: Our intake tests were conducted serially after taste-reactivity tests and so were delayed 30 min after a microinjection, whereas Mena et al. measured intake directly after microinjections. Our serial procedure avoided the need to double the number of rats, which would have been required to conduct separate food intake and taste-reactivity tests while avoiding too many microinjections in a single rat. We therefore caution that our intake results show relative site differences in intake stimulation but may not reflect absolute failures in site capacity to increase intake.

For the insula, no sites here supported reliable increases in intake after either orexin or DAMGO microinjections, in either the anterior-mid insula (hedonic coldspot) or far-posterior insula

(hedonic hotspot), although there was some variability across individual sites. However, DAMGO microinjections (although not orexin) at several sites in the piriform cortex (i.e., ventral to insula) did appear to increase intake (Figs. 6 and 7).

Discussion

Our results provide evidence that particular sites in the OFC and insula are capable of causing enhancements of sucrose hedonic impact ("liking" reactions). Further, our maps localize this capability to particular hedonic hotspots. Both the rostromedial OFC and far-caudal insula regions each contained a discrete 6–8 mm³ hedonic hotspot where mu-opioid or orexin microinjections amplified the hedonic impact of sweetness, expressed here as 200–300% increases in affective "liking" reactions elicited by sucrose taste.

The OFC hotspot lay near the anterior tip of the PFC (i.e., just caudal and dorsal to the olfactory bulb) and extended posteriorly in medial, ventral, and lateral directions to fill the rostral two-thirds of the OFC. The insula hotspot was contained in the farthest-posterior quarter of the structure. The two cortical hotspots were positioned nearly as bookends around an extended 5-mm-long coldspot strip on the lateral surface of the brain, stretching from posterior OFC to midposterior insula (18 mm³). In that hedonic coldspot lateral strip, the same neurochemical stimulations suppressed "liking" reactions to sweetness by 30–50% of control levels. DAMGO and orexin microinjections produced virtually identical maps for these cortical hedonic hotspots and the coldspot.

Cortical Involvement in Affective Processing. As noted earlier, human fMRI neuroimaging and animal electrophysiological studies have reported that midanterior OFC and insula activity encodes the pleasantness of odors and tastes, such as palatable beverages or chocolate candy (1, 3, 5, 6, 36–40). Activity in those regions even tracks alliesthesia decrements in pleasure for the same tastes induced by caloric and/or sensory-specific satiety (3, 5). Such demonstrations provide strong evidence for hedonic coding (rather than alternative coding of stable sensory features, such as sweetness) (1). Conversely, negative stimulus-evoked affect, such as disgust or pain, has been reported to correlate with anterior insula activity (41–44), whereas posterior insula activity is also reported to correlate with positive food reward (25).

Experimental stimulations of limbic cortex, mostly in animals, have also implicated the OFC and insula in causing reward functions, such as incentive motivation to consume food. For example, Mena et al. (15) demonstrated that DAMGO microinjections at sites in the ventral and medial PFC of rats increased eating behavior and intake of food. Similarly, optogenetic stimulation of a putative "sweet" gustatory cortex zone of the rostral insula in mice is reported to induce a conditioned place preference for a paired location and caused increased licking of a water spout (45). Electrical stimulation in the OFC or insula supports self-stimulation behavior in rats (46), and midinsula stimulation also produces other positive reactions such as social-affiliative behaviors in monkeys (47). By contrast, electrical stimulation specifically of the anterior insula has been reported to elicit disgust reactions in cats and monkeys (48), including actively spitting out a normally preferred food (47). In mice, optogenetic stimulation at a putative "bitter" zone in the midinsula is reported to induce disgust gapes to water (45). Finally, in humans, spontaneous electrical excitation in the anterior insula associated with epileptic seizures has been suggested to be sometimes accompanied by "ecstatic auras" involving "intense feeling of bliss, [and] enhanced well-being" (49). Collectively, these gain-of-function effects seem consistent with our findings that localized cortical site stimulations can modulate "liking" reactions.

Cross-Species Homologies. Although necessarily speculative, it seems of interest to consider what potential human cortical homologs might correspond to the hedonic hotspot or coldspot sites mapped here in rats. Several considerations suggest that a
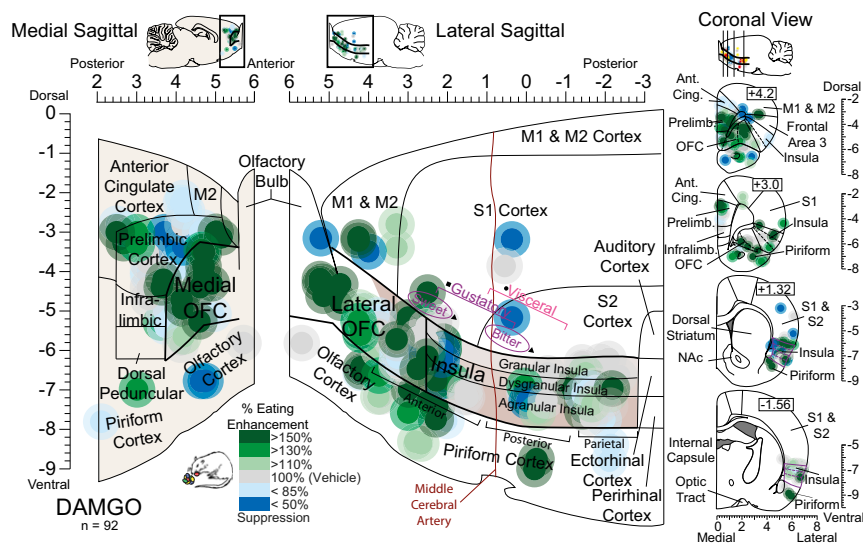
Fig. 7. Mu-opioid stimulation increases food intake in the OFC and piriform cortex. Functional maps show increases (green) or decreases (blue) in palatable food intake caused by DAMGO microinjections in cortical sites. Each symbol placement indicates a microinjection site; its size reflects Fos plume size, and the color reflects the percent change in consumption of M&Ms induced by the drug microinjection compared with vehicle control levels in the same rat. DAMGO microinjections in the medial PFC, rostromedial and caudolateral OFC, and far-anterior insula increased food intake >130% over vehicle control days [$\chi^2 = 6.632$, $P = 0.036$; $Z = -2.334$, $P = 0.020$, $r = 0.54$, CI (-0.7, 4.3)]. DAMGO microinjection in the piriform cortex also increased food intake (overall: $\chi^2 = 6.222$, $P = 0.045$; $Z = -1.886$, $P = 0.059$). No consistent increase was observed with microinjections in the middle or posterior insula ($\chi^2 = 2.78$, $P = 0.249$), even in the far-posterior hotspot ($\chi^2 = 2.516$, $P = 0.284$). Likewise, no increase was observed with microinjections in infralimbic or anterior cingulate sites ($\chi^2 = 0.187$, $P = 0.911$) or in olfactory cortex ($\chi^2 = 2.80$, $P = 0.247$) or motor/somatosensory cortex ($\chi^2 = 1.652$, $P = 0.438$).

potential human homolog to the rat anterior OFC hedonic hotspot might exist in agranular regions of the caudal OFC (i.e., Brodmann areas 14c and 13a) (50). Humans have additional rostral zones that extend further anteriorly in the OFC but are granular (Brodmann areas 10, 11, 13, 14, 12/47), whereas in rats all of the OFC is agranular, including the hedonic hotspot. Agranular cortex has been suggested to be the best candidate for primate–rodent OFC homology, and if a human hedonic hotspot were similarly agranular, it would likely be in the caudal OFC.

By comparison, the cortical hedonic coldspot strip of rats identified here (i.e., caudolateral OFC to anterior and middle insula) included granular as well as agranular regions of insula. The coldspot strip continued caudally in rats through the entire gustatory zone of the middle and posterior insula. The gustatory cortex in rats is an ~2-mm A–P strip of rostral agranular or dysgranular insula around and especially rostral to the middle artery (51–53). It was recently suggested that a specific anterior site in the gustatory insula cortex of mice codes sweet taste, whereas a specific posterior site codes bitterness (45; however, see ref. 53). Our hedonic coldspot here probably contained both those putative taste-specific sites (although our study used rats rather than mice) and extended even more posteriorly into what is traditionally classified as a visceral region of the sensory insula. Others have similarly suggested that taste-related functions may extend posteriorly beyond the classic gustatory cortex into this same traditionally visceral insula region. For example, Schier et al. (13) showed that lesions in the insula disrupted Pavlovian taste-aversion learning (caused by pairing a novel taste with LiCl-induced nausea). Their taste-aversion disruptive zone in the insula approximately straddled the border between our insula coldspot and insula hotspot (54).

In primates, the gustatory cortex is in the rostral insula and frontal operculum (52, 55, 56). In humans, potential comparison is further complicated by considering that human insula has more recognized subregions than rat insula (57, 58) and that the human orientation of agranular, dysgranular, and granular zones of insula appears to be rotated by nearly 45° clockwise compared with rats.

Thus, the agranular zone is located anteriorly (and ventrally) in human insula, whereas the granular zone is posterior (and dorsal). By comparison, in rats the agranular zone is more simply the ventral insula, and the granular zone is the dorsal insula. Here, our insula hedonic coldspot included all granular, dysgranular, and granular zones of the anterior and midposterior rat insula. The caudal tip of our insula hedonic hotspot is so far posterior that this region was not even recognized as belonging to rodent insula until the 1990s (59). Its reclassification as insula was based on the recognition that it received afferent visceral sensory inputs, contained agranular, dysgranular, and granular zones, and sent efferent projections to amygdala, all similar to other insula regions (60). We suggest speculatively that, if a rat hedonic coldspot or hotspot were rotated similarly to the human rotation of insula granularity zones, then a corresponding human hedonic coldspot/hotspot might comprise an anterior subregion of agranular insula, an anterior subregion of dysgranular insula, and even an anterior subregion of granular insula (even though the human granular zone is posterior to agranular/dysgranular zones). Alternatively, if simple anterior versus posterior placement in insula matters more than zone rotation in hedonic organization, then the entire human agranular insula (i.e., anterior insula) might belong to a hedonic coldspot, whereas dysgranular or granular insula might contain the human hedonic hotspot (i.e., posterior insula). Future studies may be able to assess such possibilities.

Gain Versus Loss of Function. Our finding that cortical hedonic hotspot stimulations caused gains of "liking" function does not necessarily imply that lesions of the same cortical hotspots would produce deficits in "liking" or losses of hedonic function (7–12, 14, 61). In particular, gains of function can exist without reciprocal loss of function, especially for structures that occupy relatively high levels in a brain control hierarchy (62, 63). High levels of a hierarchy may potentiate functions that are largely embedded in lower structures to produce gains of function. However, damage to those higher structures would produce loss of hierarchical control but not loss of original functions remaining in lower structures.
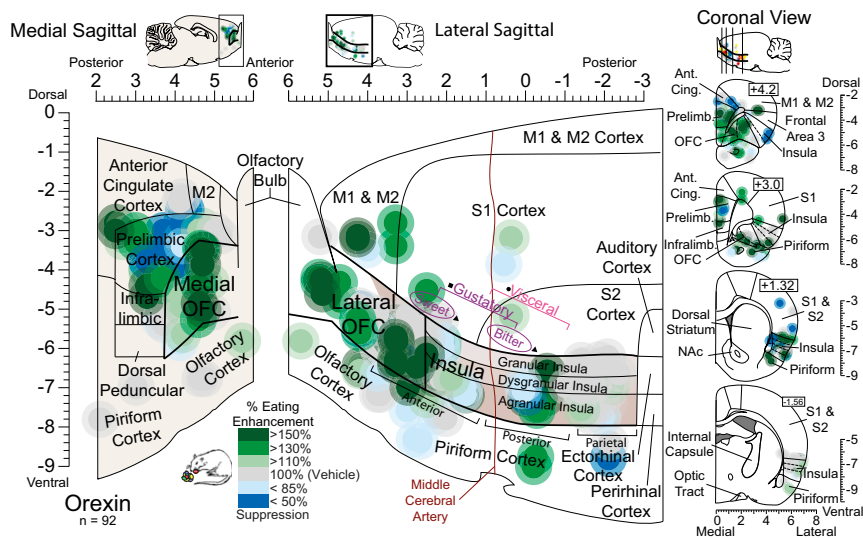
Fig. 8. Orexin stimulation in the OFC increases food intake. Functional maps show increases (green) or decreases (blue) in palatable food intake caused by orexin microinjections in cortical sites. Symbols are as in Fig. 7. The color reflects the percent change in the consumption of M&Ms induced by the orexin microinjection compared with vehicle control levels in the same rat. Orexin microinjections in all OFC regions increased food intake by 150% over vehicle control levels [$\chi^2 = 6.632$, $P = 0.036$; $Z = -2.175$, $P = 0.030$, $r = 0.50$, CI (0.7, 2.7)], as well as in a few medial prefrontal sites in the anterior cingulate and infralimbic cortex. No consistent increase was observed after orexin microinjections in any region of the insula ($\chi^2 = 2.78$, $P = 0.249$; $\chi^2 = 2.516$, $P = 0.284$). Likewise, no intake increase was observed after orexin microinjections at sites in the piriform cortex ($Z = 0.471$, $P = 0.637$), ventromedial PFC ($\chi^2 = 0.187$, $P = 0.911$), olfactory cortex ($\chi^2 = 2.80$, $P = 0.247$), or motor/somatosensory cortex ($\chi^2 = 1.652$, $P = 0.438$).

These considerations may help explain why cortical lesions of the hedonic hotspot/coldspot sites identified here have generally failed to impair measures of food reward (12, 14, 61, 64). Similarly, human patients with extensive damage to OFC and insula appear to remain capable of normal hedonic reactions to many pleasant versus unpleasant stimuli (9, 10). For example, one such patient with extensive damage to both the OFC and insula still "... readily displays signs of positive emotion including happiness, amusement, interest, and excitement" (9). By contrast, cortical lesions do appear to cause subtle taste-specific alterations in sensory preference or detection, and lesions of the posterior insula can disrupt learning of conditioned taste aversions (54).

Similar to OFC and insula hotspots, the NAc hedonic hotspot in the rostromedial shell provides another subcortical example of gain without loss of hedonic function: Opioid/orexin stimulation enhances "liking", but lesions do not impair "liking" reactions. By contrast, the caudal VP hotspot combines both gain of function and loss of function for hedonic causation, as lesions there abolish normal "liking" reactions so that sweet tastes elicit disgust reactions (16, 17, 26, 65, 66). Even suppression of "liking" by opioid/orexin stimulation of a cortical OFC–insula coldspot or a caudal shell NAc coldspot may be viewed as essentially a gain of function, via recruiting active hedonic-suppression circuitry to reduce "liking" reactions. In short, we view cortical hedonic hotspots/coldspots as specifically gain-of-function mechanisms, so that damage to them need not necessarily be expected to cause hedonic changes.

Brain-Wide Circuitry for Hedonic Enhancement vs. Suppression. Consistent with this view, we found that opioid/orexin stimulation in cortical hotspots recruited distinct patterns of Fos activation across the brain, in other cortical regions, and in several subcortical structures that contain other hedonic hotspots. By contrast, cortical coldspot stimulation recruited a very different pattern of Fos activation across the brain, including other hedonic coldspots, that might mediate active suppression of "liking" reactions.

For example, DAMGO and orexin microinjections in the OFC or insula hotspots typically increased Fos expression in the corresponding cortical hotspot. They also increased Fos in two

subcortical hotspots: the NAc (the rostrodorsal quadrant of the medial shell) and VP (the posterior/dorsolateral half of the VP) (31, 67). This recruitment of distant hotspots seems similar to previous findings that NAc hotspot stimulation recruited VP hotspot activation, and vice versa (33). Mutual recruitment among hotspots suggests that neurochemical stimulation of a given hedonic hotspot recruits other hotspots into simultaneous unanimous activation, forming an integrated network of hedonic circuitry activation.

In contrast, DAMGO/orexin microinjections in the cortical coldspot caused a suppression of Fos in the OFC hotspot, suggesting intercortical suppression as one mechanism to reduce hedonic impact. Additionally, increased Fos was observed in the caudal NAc coldspot, perhaps indicating an active hedonic-suppression circuit.

That valence difference between circuitry activated by stimulation of cortical hedonic hotspots versus the hedonic coldspot was the most striking feature observed in brain Fos patterns, but there were also differences in the activation patterns of the two cortical hotspots. For example, only OFC hotspot stimulation increased Fos in the lateral hypothalamus, potentially suggesting an interaction basis for hedonic modulation by physiological hunger and satiety states. Conversely, insula hotspot stimulations increased Fos in the anterior portion of the VP, where opioid stimulation can negatively suppress hedonic "liking" reactions but where other manipulations stimulate appetitive motivation for food or drug rewards (31, 32). All these Fos changes occurred even in the absence of taste-elicited reactions, which helps to rule out any possibility that they were motor consequences of behavioral feedback from orofacial reactions and indicates instead that circuitry patterns were directly activated by neurochemical stimulation of the cortical sites.

Conclusion. Our results indicate that opioid/orexin stimulation of particular cortical sites recruits brain-wide hedonic circuitry to either enhance or suppress the positive hedonic impact of sweetness. The OFC and insula each contain a distinct and localized hedonic hotspot where mu-opioid or orexin stimulations amplify "liking" reactions to sucrose taste. Conversely, an

anatomically intervening strip forms a hedonic coldspot where the same neurochemical stimulations suppress "liking". OFC hotspot stimulations also enhanced voluntary food intake, but insula hotspot stimulations did not. Additionally, other cortical sites stimulated intake, including sites in piriform cortex and in the OFC coldspot. Thus, there is overlap, but there also are differences, between cortical localization of circuitry that modulates hedonic impact and mechanisms that contribute to the motivation to eat. A better understanding of cortical hedonic modulation may have implications for understanding the hierarchical neural organization of affective disorders as well as of normal "liking" reactions.

Materials and Methods

Animals. One hundred twenty-four Sprague–Dawley rats (250–400 g; male: $n = 68$, female: $n = 56$; behavioral test groups: $n = 92$; cortical Fos plume groups: $n = 32$) were housed in a reverse 12-h light/dark cycle at 21 °C constant temperature. Chow and water were provided ad libitum. All procedures were approved by the Institutional Animal Care and Use Committee at the University of Michigan.

Taste Reactivity and Cannulation Surgery. Rats were anesthetized with ketamine hydrochloride (80 mg/kg, i.p.) mixed with xylazine (5 mg/kg, i.p.) and were pretreated with atropine (0.05 mg/kg, i.p.) to prevent respiratory distress. Rats were implanted with microinjection guide cannulas in the cortex, with sites chosen so that the group as a whole would blanket the OFC, medial PFC, and insula. Each rat was placed in a stereotaxic apparatus (David Kopf Instruments) with the incisor bar set at −3.3 mm below intraoral zero for flat skull measurements. Bilateral permanent microinjection guide cannulas were implanted (23-gauge, stainless steel; length = 12.5 mm for OFC and medial prefrontal sites, 14 mm for insula sites). Bilateral placements were aimed to be symmetrical across sides within each rat, with identical mirror coordinates on left/right hemispheres. OFC placements ($n = 19$) ranged from +5.64 mm to +2.76 mm (A–P) from Bregma, ±0.2 mm to ±3.4 mm M–L, and −4.0 mm to −6.8 mm D–V. Insula placements ($n = 32$) ranged from +4.2 mm to −2.64 mm (A–P) from Bregma, ±3.5 mm to ±6.6 mm M–L, and −5.6 mm to −7.8 mm D–V. Microinjection guide cannulas were anchored to the skull using surgical screws and dental acrylic and were plugged with 28-gauge stainless-steel obturators to prevent clogging. In the same surgery, rats intended for behavioral taste-reactivity testing also were implanted with bilateral oral cannulas (polyethylene-100 tubing) to permit oral infusions of sucrose and quinine solutions (67). Oral cannulas entered the mouth in the upper cheek pouch lateral to the first maxillary molar, ascended beneath the zygomatic arch, and then exited through the skin at the dorsal headcap (68). After surgery, each rat received s.c. injections of carprofen (5 mg/kg) for pain relief and another carprofen dose 24 h later. Rats recovered for 1 wk before beginning behavioral testing.

Drug Microinjections. Rats were handheld in the lap of the experimenter during bilateral microinjections. Obturators were removed, microinjection cannulas were inserted into guide cannulas [OFC: 12.5 mm, 29-gauge; insula: 14 mm, 29-gauge; calibrated so that the microinjection cannula extended 1 mm (OFC) or 2 mm (insula) beyond its guide cannula], and the syringe pump was connected to the microinjection cannula with PE-50 polyethylene tubing. Drug and vehicle solutions were previously frozen and brought to room temperature (∼21 °C) immediately before microinjection. Each test day a rat received bilateral microinjections of (i) DAMGO, a selective mu receptor agonist, at a dose of 0.05 μg/0.2 μL per side dissolved in artificial cerebrospinal fluid (ACSF); or (ii) Orexin-A, an excitatory neuropeptide hormone, at 500 pmol/0.2 μL per side; or (iii) vehicle ACSF alone at 0.2 μL per side as a control condition. Each rat received each drug or vehicle condition on different days, one condition per day, counterbalanced across rats. Doses of DAMGO and orexin were based on previous studies demonstrating effective affective modulation (16, 26, 69, 70). Drugs were microinjected over a 1-min period at a volume of 0.2 μL per side at a speed of 0.2 μL/min by syringe pump. After each microinjection, injectors were left in place for 1 min to allow for drug diffusion, after which obturators were

replaced. Rats then were immediately placed in the taste-reactivity testing chamber for 25 min before oral infusions.

Taste-Reactivity Tests. Rats were each handled and habituated to the testing conditions for 25 min on four consecutive days before any microinjections or tests, and they received a mock injection of vehicle (ACSF) on the fourth day of habituation. The taste-reactivity test (68, 71, 72) was used to elicit and measure affective orofacial reactions to either sucrose solution (1 mL of 1.0% or 0.029 M concentration) or quinine solution (1 mL of 3×10^{-3} M). This sucrose concentration was relatively low to facilitate detection of hedonic increases induced by drug microinjections (i.e., to avoid ceiling effects), whereas the quinine concentration was relatively high to elicit robust disgust reactions so that potential aversive reductions induced by drugs could be detected. Sucrose or quinine solutions were infused via tubing (PE-50 connected to a PE-10 delivery nozzle) connected to one of the rat's oral cannulas via syringe pump. Twenty-five minutes after cortical microinjection, the sucrose solution was infused evenly over a 1-min period. After a 5-min delay, quinine solution began to be infused intraorally for a 1-min taste-reactivity test. Orofacial taste reactivity to sucrose and quinine solutions was videorecorded via a close-up lens aimed at an angled mirror placed underneath the transparent floor to capture a clear view of the mouth and ventral face and saved for subsequent video analysis (*Supporting Information*) (73).

Food Intake Tests. A voluntary 1-h test of palatable food intake was run beginning ∼30 min after the taste-reactivity test on each day. For intake tests rats were transferred to another 23 × 20 × 45 cm chamber that contained a 1-cm layer of corncob bedding (rats had been previously habituated to the food intake chamber during the four habituation days). Each rat was given free access to ∼20 g preweighed palatable milk-chocolate candy (M&Ms, 20 candies) and a water bottle. Chocolates were weighed before and after testing to calculate the amount consumed. Behavior during the 1-h test was videorecorded and later scored for eating behavior (duration in seconds), water drinking behavior (in seconds), grooming behavior (in seconds), and for food investigatory sniffs, food carrying, cage crosses, and rears (number of bouts).

Histology and Fos-Like Protein Immunohistochemistry. After the last day of behavioral testing, rats were deeply anesthetized with an overdose of sodium pentobarbital and were decapitated. Brains were extracted and fixed in 10% paraformaldehyde solution for 1–2 d followed by a 25% sucrose solution in 0.1 M NaPB for 2–3 d. For histological analysis of cannula placements in behaviorally tested animals, brains were sliced in 60-μm sections for regions of interest on a cryostat and then were mounted, dried, and stained with cresyl violet. Microscope inspection determined the center of each microinjection site, and the position was mapped on a stereotaxic atlas (27). Rats that were used for Fos analyses were anesthetized and transcardially perfused 90 min after receiving a microinjection of vehicle, orexin, or DAMGO. Brains were sliced at 40-μm increments, and samples were collected from the cortical injection site as well as from the other cortical and subcortical sites of interest (*SI Materials and Methods*). Samples were processed for Fos-like immunoreactivity using normal donkey serum, goat anti–c-fos (Santa Cruz Biotechnology), and donkey anti-goat Alexa Fluor 594 (Invitrogen). Injection sites were scattered across the OFC and insula to develop a single representative "cortical plume." Sections were mounted, air-dried, and cover-slipped with Prolong Gold antifade reagent (Invitrogen). Zones that showed elevated expression of fluorescent Fos in the neurons surrounding the microinjection sites were then assessed via microscope along radial arms composed of 50 × 50 μm boxes (26, 74). Distant Fos quantification is described in *Supporting Information*.

1. Berridge KC, Kringelbach ML (2015) Pleasure systems in the brain. *Neuron* 86:646–664.
2. Castro DC, Berridge KC (2014) Advances in the neurobiological bases for food 'liking' versus 'wanting'. *Physiol Behav* 136:22–30.
3. Kringelbach ML, O'Doherty J, Rolls ET, Andrews C (2003) Activation of the human orbitofrontal cortex to a liquid food stimulus is correlated with its subjective pleasantness. *Cereb Cortex* 13:1064–1071.
4. Kringelbach ML, Rolls ET (2004) The functional neuroanatomy of the human orbitofrontal cortex: Evidence from neuroimaging and neuropsychology. *Prog Neurobiol* 72:341–372.
5. Rolls ET, Kringelbach ML, de Araujo IET (2003) Different representations of pleasant and unpleasant odours in the human brain. *Eur J Neurosci* 18:695–703.
6. Small DM, Zatorre RJ, Dagher A, Evans AC, Jones-Gotman M (2001) Changes in brain activity related to eating chocolate: From pleasure to aversion. *Brain* 124:1720–1733.

7. Beer JS, Heerey EA, Keltner D, Scabini D, Knight RT (2003) The regulatory function of self-conscious emotion: Insights from patients with orbitofrontal damage. *J Pers Soc Psychol* 85:594–604.

8. Bramham J, Morris RG, Hornak J, Bullock P, Polkey CE (2009) Social and emotional functioning following bilateral and unilateral neurosurgical prefrontal cortex lesions. *J Neuropsychol* 3:125–143.

9. Feinstein JS, et al. (2010) Bilateral limbic system destruction in man. *J Clin Exp Neuropsychol* 32:88–106.

10. Philippi CL, et al. (2012) Preserved self-awareness following extensive bilateral brain damage to the insula, anterior cingulate, and medial prefrontal cortices. *PLoS One* 7: e38413.

11. Szczepanski SM, Knight RT (2014) Insights into human behavior from lesions to the prefrontal cortex. *Neuron* 83:1002–1018.

12. Bales MB, Schier LA, Blonde GD, Spector AC (2015) Extensive gustatory cortex lesions significantly impair taste sensitivity to KCl and quinine but not to sucrose in rats. *PLoS One* 10:e0143419.

13. Schier LA, Hashimoto K, Bales MB, Blonde GD, Spector AC (2014) High-resolution lesion-mapping strategy links a hot spot in rat insular cortex with impaired expression of taste aversion learning. *Proc Natl Acad Sci USA* 111:1162–1167.

14. Wirsig CR, Grill HJ (1982) Contribution of the rat's neocortex to ingestive control: I. Latent learning for the taste of sodium chloride. *J Comp Physiol Psychol* 96:615–627.

15. Mena JD, Sadeghian K, Baldo BA (2011) Induction of hyperphagia and carbohydrate intake by μ-opioid receptor stimulation in circumscribed regions of frontal cortex. *J Neurosci* 31:3249–3260.

16. Castro DC, Terry RA, Berridge KC (2016) Orexin in rostral hotspot of nucleus accumbens enhances sucrose 'liking' and intake but scopolamine in caudal shell shifts 'liking' toward 'disgust' and 'fear'. *Neuropsychopharmacology* 41:2101–2111.

17. Ho C-Y, Berridge KC (2013) An orexin hotspot in ventral pallidum amplifies hedonic 'liking' for sweetness. *Neuropsychopharmacology* 38:1655–1664.

18. Berthoud H-R, Münzberg H (2011) The lateral hypothalamus as integrator of metabolic and environmental needs: From electrical self-stimulation to opto-genetics. *Physiol Behav* 104:29–39.

19. Mahler SV, Moorman DE, Smith RJ, James MH, Aston-Jones G (2014) Motivational activation: A unifying hypothesis of orexin/hypocretin function. *Nat Neurosci* 17: 1298–1303.

20. Pinos H, Pérez-Izquierdo MA, Carrillo B, Collado P (2011) Effects of undernourishment on the hypothalamic orexinergic system. *Physiol Behav* 102:17–21.

21. Berridge CW, España RA, Vittoz NM (2010) Hypocretin/orexin in arousal and stress. *Brain Res* 1314:91–102.

22. Jin J, et al. (2016) Orexin neurons in the lateral hypothalamus project to the medial prefrontal cortex with a rostro-caudal gradient. *Neurosci Lett* 621:9–14.

23. Peyron C, et al. (1998) Neurons containing hypocretin (orexin) project to multiple neuronal systems. *J Neurosci* 18:9996–10015.

24. Hollander JA, Lu Q, Cameron MD, Kamenecka TM, Kenny PJ (2008) Insular hypocretin transmission regulates nicotine reward. *Proc Natl Acad Sci USA* 105:19480–19485.

25. Simmons WK, et al. (2013) Category-specific integration of homeostatic signals in caudal but not rostral human insula. *Nat Neurosci* 16:1551–1552.

26. Castro DC, Berridge KC (2014) Opioid hedonic hotspot in nucleus accumbens shell: Mu, delta, and kappa maps for enhancement of sweetness "liking" and "wanting". *J Neurosci* 34:4239–4250.

27. Paxinos G, Watson C (2007) *The Rat Brain in Stereotaxic Coordinates* (Elsevier, Amsterdam).

28. Cechetto DF, Saper CB (1987) Evidence for a viscerotopic sensory representation in the cortex and thalamus in the rat. *J Comp Neurol* 262:27–45.

29. Shi CJ, Cassell MD (1998) Cortical, thalamic, and amygdaloid connections of the anterior and posterior insular cortices. *J Comp Neurol* 399:440–468.

30. Mahler SV, Smith KS, Berridge KC (2007) Endocannabinoid hedonic hotspot for sensory pleasure: Anandamide in nucleus accumbens shell enhances 'liking' of a sweet reward. *Neuropsychopharmacology* 32:2267–2278.

31. Smith KS, Berridge KC (2005) The ventral pallidum and hedonic reward: Neurochemical maps of sucrose "liking" and food intake. *J Neurosci* 25:8637–8649.

32. Mahler SV, et al. (2014) Designer receptors show role for ventral pallidum input to ventral tegmental area in cocaine seeking. *Nat Neurosci* 17:577–585.

33. Smith KS, Berridge KC (2007) Opioid limbic circuit for reward: Interaction between hedonic hotspots of nucleus accumbens and ventral pallidum. *J Neurosci* 27: 1594–1605.

34. Castro DC, Cole SL, Berridge KC (2015) Lateral hypothalamus, nucleus accumbens, and ventral pallidum roles in eating and hunger: Interactions between homeostatic and reward circuitry. *Front Syst Neurosci* 9:90.

35. Selleck RA, Baldo BA (2017) Feeding-modulatory effects of mu-opioids in the medial prefrontal cortex: A review of recent findings and comparison to opioid actions in the nucleus accumbens. *Psychopharmacology (Berl)* 234:1439–1449.

36. Hosokawa T, Kato K, Inoue M, Mikami A (2007) Neurons in the macaque orbitofrontal cortex code relative preference of both rewarding and aversive outcomes. *Neurosci Res* 57:434–445.

37. Kringelbach ML (2005) The human orbitofrontal cortex: Linking reward to hedonic experience. *Nat Rev Neurosci* 6:691–702.

38. Roesch MR, Olson CR (2004) Neuronal activity related to reward value and motivation in primate frontal cortex. *Science* 304:307–310.

39. Segerdahl AR, Mezue M, Okell TW, Farrar JT, Tracey I (2015) The dorsal posterior insula subserves a fundamental role in human pain. *Nat Neurosci* 18:499–500.

40. Tremblay L, Schultz W (1999) Relative reward preference in primate orbitofrontal cortex. *Nature* 398:704–708.

41. Calder AJ, et al. (2007) Disgust sensitivity predicts the insula and pallidal response to pictures of disgusting foods. *Eur J Neurosci* 25:3422–3428.

42. Lamm C, Silani G, Singer T (2015) Distinct neural networks underlying empathy for pleasant and unpleasant touch. *Cortex* 70:79–89.

43. Mataix-Cols D, et al. (2008) Individual differences in disgust sensitivity modulate neural responses to aversive/disgusting stimuli. *Eur J Neurosci* 27:3050–3058.

44. Wager TD, et al. (2004) Placebo-induced changes in FMRI in the anticipation and experience of pain. *Science* 303:1162–1167.

45. Peng Y, et al. (2015) Sweet and bitter taste in the brain of awake behaving animals. *Nature* 527:512–515.

46. Routtenberg A, Sloan M (1972) Self-stimulation in the frontal cortex of Rattus norvegicus. *Behav Biol* 7:567–572.

47. Caruana F, Jezzini A, Sbriscia-Fioretti B, Rizzolatti G, Gallese V (2011) Emotional and social behaviors elicited by electrical stimulation of the insula in the macaque monkey. *Curr Biol* 21:195–199.

48. Hess WR, Akert K, McDonald DA (1952) Functions of the orbital gyri of cats. *Brain* 75: 244–258.

49. Picard F, Craig AD (2009) Ecstatic epileptic seizures: A potential window on the neural basis for human self-awareness. *Epilepsy Behav* 16:539–546.

50. Wallis JD (2011) Cross-species studies of orbitofrontal cortex and value-based decision-making. *Nat Neurosci* 15:13–19.

51. Kosar E, Grill HJ, Norgren R (1986) Gustatory cortex in the rat. I. Physiological properties and cytoarchitecture. *Brain Res* 379:329–341.

52. Small DM (2006) Central gustatory processing in humans. *Adv Otorhinolaryngol* 63: 191–220.

53. Fletcher ML, Ogg MC, Lu L, Ogg RJ, Boughter JD, Jr (2017) Overlapping representation of primary tastes in a defined region of the gustatory cortex. *J Neurosci* 37:7595–7605.

54. Schier LA, Blonde GD, Spector AC (2016) Bilateral lesions in a specific subregion of posterior insular cortex impair conditioned taste aversion expression in rats. *J Comp Neurol* 524:54–73.

55. Ongür D, Price JL (2000) The organization of networks within the orbital and medial prefrontal cortex of rats, monkeys and humans. *Cereb Cortex* 10:206–219.

56. Price JL (2007) Definition of the orbital cortex in relation to specific connections with limbic and visceral structures and other cortical regions. *Ann N Y Acad Sci* 1121:54–71.

57. Nieuwenhuys R (2012) The insular cortex: A review. *Prog Brain Res* 195:123–163.

58. Rose M (1928) Die inselrinde des menschen und der tiere. *J Psychol Neurol* 37:467–624.

59. Paxinos G, Watson C (1998) *The Rat Brain Atlas in Stereotaxic Coordinates* (Academic, San Diego).

60. Shi CJ, Cassell MD (1998) Cascade projections from somatosensory cortex to the rat basolateral amygdala via the parietal insular cortex. *J Comp Neurol* 399:469–491.

61. King CT, Hashimoto K, Blonde GD, Spector AC (2015) Unconditioned oromotor taste reactivity elicited by sucrose and quinine is unaffected by extensive bilateral damage to the gustatory zone of the insular cortex in rats. *Brain Res* 1599:9–19.

62. Jackson JH (1958) *Selected Writings of John Hughlings Jackson* (Staples, London). Available at https://scholar.google.com/scholar?cluster=3317313759043458542&hl=en&oi=scholarr. Accessed September 25, 2017.

63. Gallistel CR (2013) *The Organization of Action: A New Synthesis* (Psychology) (Lawrence Erlbaum, Hillsdale, NJ).

64. Braun JJ, Lasiter PS, Kiefer SW (1982) The gustatory neocortex of the rat. *Physiol Psychol* 10:13–45.

65. Cromwell HC, Berridge KC (1993) Where does damage lead to enhanced food aversion: The ventral pallidum/substantia innominata or lateral hypothalamus? *Brain Res* 624:1–10.

66. Ho C-Y, Berridge KC (2014) Excessive disgust caused by brain lesions or temporary inactivations: Mapping hotspots of the nucleus accumbens and ventral pallidum. *Eur J Neurosci* 40:3556–3572.

67. Peciña S, Berridge KC (2005) Hedonic hot spot in nucleus accumbens shell: Where do mu-opioids cause increased hedonic impact of sweetness? *J Neurosci* 25:11777–11786.

68. Grill HJ, Norgren R (1978) The taste reactivity test. I. Mimetic responses to gustatory stimuli in neurologically normal rats. *Brain Res* 143:263–279.

69. Smith KS, Berridge KC, Aldridge JW (2011) Disentangling pleasure from incentive salience and learning signals in brain reward circuitry. *Proc Natl Acad Sci USA* 108: E255–E264.

70. Thorpe AJ, Kotz CM (2005) Orexin A in the nucleus accumbens stimulates feeding and locomotor activity. *Brain Res* 1050:156–162.

71. Steiner JE, Glaser D, Hawilo ME, Berridge KC (2001) Comparative expression of hedonic impact: Affective reactions to taste by human infants and other primates. *Neurosci Biobehav Rev* 25:53–74.

72. Faure A, Reynolds SM, Richard JM, Berridge KC (2008) Mesolimbic dopamine in desire and dread: Enabling motivation to be generated by localized glutamate disruptions in nucleus accumbens. *J Neurosci* 28:7184–7192.

73. Berridge KC (2000) Measuring hedonic impact in animals and infants: Microstructure of affective taste reactivity patterns. *Neurosci Biobehav Rev* 24:173–198.

74. Richard JM, Berridge KC (2013) Prefrontal cortex modulates desire and dread generated by nucleus accumbens glutamate disruption. *Biol Psychiatry* 73:360–370.